PROCEEDINGS OF SCIENCE

Jet fragmentation in two-particle correlations in pp, p–Pb and Pb–Pb collisions

M. Vargyas for the ALICE collaboration*
University of Jyväskylä and Helsinki Institute of Physics, Finland
E-mail: marton.vargyas@cern.ch

The per-trigger normalized associated particle yield as a function of the pseudorapidity difference ($\Delta\eta$) was measured in Pb–Pb and pp collisions at $\sqrt{s_{\rm NN}} = 2.76$ TeV. For the transverse momentum of the trigger hadron $8 < p_{\rm T,trig} < 15$ GeV/c and the associated hadron $6 < p_{\rm T,assoc} < 8$ GeV/c it is observed that the near side peak is narrower in central Pb–Pb collisions relative to the pp results. In peripheral Pb–Pb collisions, the near side peak width is comparable with pp. Furthermore, a detailed study is presented on the jet fragmentation transverse momentum distribution in p–Pb and pp collisions at $\sqrt{s_{\rm NN}} = 5.02$ TeV and $\sqrt{s} = 7$ TeV, respectively. The distribution exhibits two components, narrow and wide, that can be associated with hadronization and QCD radiation components in the jet fragmentation process, respectively. The shapes of these components measured in pp and p–Pb collisions agree within the experimental uncertainties.

12th International Workshop on High-pT Physics in the RHIC/LHC Era
2-5 October, 2017
University of Bergen, Bergen, Norway

*Speaker.

PoS(High-pT2017)038

1. Introduction

Ultra-relativistic heavy-ion collisions probe the strongly interacting matter in the regime of high energy densities and temperatures, where ordinary nuclear matter changes to a quark–gluon plasma (QGP). Jet quenching is a clear signature of this created new medium [1, 2]. A comparison of jet production in heavy-ion and pp collisions provides a rich source of information on the interaction of partons with the QGP. The traditional jet reconstruction tools are difficult to use in the momentum range of this analysis. Two-particle correlations provide an alternative way to study jets in this low- and intermediate-transverse momentum (p_{T}) regime. This article reports on two such measurements: (I) the analysis of the longitudinal jet-shape modification in pseudorapidity and (II) the study of the hard and soft components of QCD radiation from the analysis of the jet fragmentation transverse momentum distributions.

The analysis of the longitudinal jet-shape modification was carried out in Pb–Pb and pp collisions at $\sqrt{s_{\mathrm{NN}}}$ = 2.76 TeV, by measuring the pseudorapidity ($\Delta\eta$) and azimuthal angle ($\Delta\varphi$) differences between trigger and associated particles. The jet fragmentation is manifested as a peak around $(\Delta\eta,\Delta\varphi) = (0,0)$. The jet-shape modification was studied widely. The STAR collaboration reported no significant dependence of the jet-shape on the system size [3], confirming the assumption that the peak is indeed a result of jet fragmentation. A previous ALICE measurement [4] reported a broadening at lower transverse momentum $p_{\mathrm{T,trig}} < 6$ GeV/c and no modification in the range $6 < p_{\mathrm{T,trig}} < 8$ GeV/c.

The second part focuses on the jet fragmentation in p–Pb and pp collisions at $\sqrt{s_{\mathrm{NN}}}$ = 5.02 TeV and $\sqrt{s}$ = 7 TeV, respectively, and separates experimentally the two phases of fragmentation; the QCD branching (perturbative QCD) and the hadronization process. The hadronization-only phase shows a clear Gaussian shape, while the QCD showering part exhibits a wide, non-Gaussian one. The width of the narrow component depends only weakly on the transverse momentum of the trigger particle, while the wide component shows a rising trend, suggesting more branching at higher transverse momentum. The results are compared to both earlier measurements (CCOR [5] and PHENIX [6]) and Monte Carlo (MC) simulations (PYTHIA 8 [7], Herwig 7 [8, 9]).

2. Jet shape modification with two-particle correlations in Pb–Pb collisions

With two-particle correlation measurements low energy jets can be studied on a statistical basis. This makes the background subtraction easier. The basic quantities are the azimuthal angle difference of the so-called trigger and associated hadrons, ($\Delta\varphi = \varphi_{\mathrm{assoc}} - \varphi_{\mathrm{trig}}$) and the pseudorapidity difference ($\Delta\eta = \eta_{\mathrm{assoc}} - \eta_{\mathrm{trig}}$) of the two hadrons. From these one can construct a correlation function (Eq. 2.1), which is then corrected for experimental effects. The per-trigger normalized yield of associated particles needs to be corrected for single particle efficiency and for the geometrical pair acceptance. The latter correction is done using the mixed event technique, where as opposed to collecting pairs from the same event (N_{same}), the two particles of a pair are collected from different events (N_{mixed}). This then provides a correction that accounts for the trivial geometrical pair-acceptance along with detector effects such as spatially varying inefficiencies

$$Y(\Delta\eta) = C_{\mathrm{single}}(p_{\mathrm{T,assoc}})\frac{1}{N_{\mathrm{trig}}}\frac{\mathrm{d}N_{\mathrm{same}}/\mathrm{d}\Delta\eta}{B\cdot\mathrm{d}N_{\mathrm{mixed}}/\mathrm{d}\Delta\eta} = C_{\mathrm{single}}(p_{\mathrm{T,assoc}})\frac{1}{N_{\mathrm{trig}}}\frac{\mathrm{d}N}{\mathrm{d}\Delta\eta}, \tag{2.1}$$

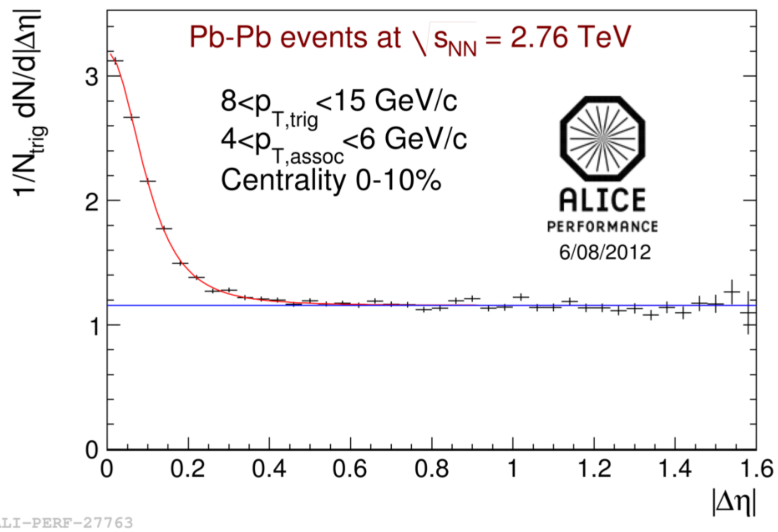

Figure 1: Example of the per-trigger yield with the background estimate of Eq. 2.1.

where $C_{\text{single}}(p_{\text{T,assoc}})$ denotes the single particle detection efficiency correction factor for the associated particles. The mixed event normalization, B, is chosen such that the mixed event distribution is 1 at $(\Delta\eta, \Delta\varphi) = (0, 0)$. After the efficiency and mixed event correction, the correlation function is symmeterized $(Y(\Delta\eta) \rightarrow Y(|\Delta\eta|))$. An example of this per-trigger yield is shown in Fig. 1. A constant background arises if the trigger and the associated particle are uncorrelated, i.e., if one of the two particles comes from the underlying event. In order to remove the background component, the per-trigger yield was fitted with a Kaplan function plus a constant. Once the background is removed, the medium induced modification of the near side jet can be studied by means of the ratio

$$I_{\text{AA}}(|\Delta\eta|) = \frac{Y^{\text{Pb-Pb}}|(\Delta\eta|)}{Y^{\text{pp}}(|\Delta\eta|)}, \tag{2.2}$$

i.e., the ratio of the yield in Pb–Pb to the yield in pp collisions measured at the same center of mass collision energy. This quantity is sensitive to the modification of the jet shape, and it shows a falling trend in case of narrowing, a rising trend for broadening, and would be a constant in case of no shape modification.

Figure 2 shows I_{AA} as a function of $|\Delta\eta|$ using the $8 < p_{\text{T,trig}} < 15$ GeV/c charged hadron trigger. The color boxes around the data points show the point to point uncorrelated systematic uncertainty, and the gray band shows the scaling (i.e. correlated) systematic uncertainty.

Comparing the shape of this peak measured in Pb–Pb collision with the corresponding pp peak, one observes a narrowing in pseudorapidity in the $8 < p_{\text{T,trig}} < 15$ GeV/c (high-p_{T}) region, while no modification is visible in the $6 < p_{\text{T,trig}} < 8$ GeV/c (intermediate-p_{T}) region. This narrowing effect is prominent in central collisions and it vanishes in peripheral collisions. This result agrees with the previous ALICE measurement [4], as the narrowing is observed only at higher p_{T}, $8 < p_{\text{T,trig}} < 15$ GeV/c.

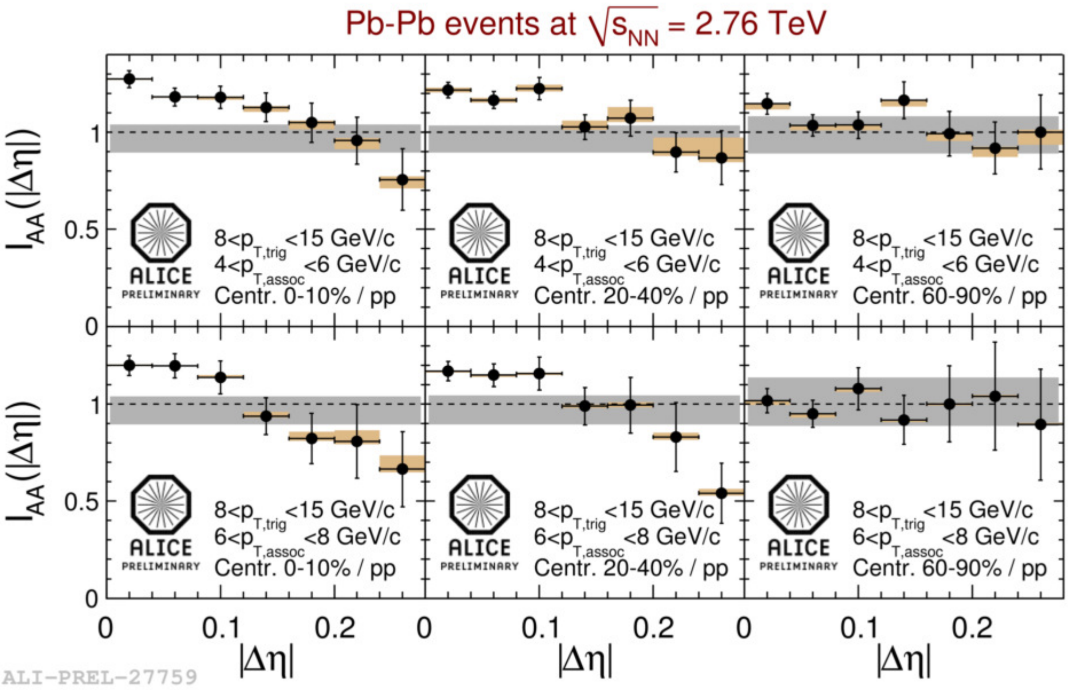

Figure 2: I_{AA} as a function of $|\Delta\eta|$ measured for $8 < p_{T,trig} < 15$ GeV/c with $4 < p_{T,assoc.} < 6$ GeV/c (top row), and $6 < p_{T,assoc.} < 8$ GeV/c (bottom row). The centrality percentile of Pb–Pb collisions grows from left to right, 0–10%, 20–40% and 60–90%, respectively. The gray band shows the scaling uncertainty. The color boxes around the data points show point to point uncorrelated systematic uncertainty.

3. Jet fragmentation transverse momentum distributions

The jet fragmentation transverse momentum, j_T, has been studied extensively [5, 6, 10, 11, 12]. Based on PYTHIA [7] studies, it is assumed that the j_T distributions can be decomposed into a sum of two components reflecting hadronization and soft QCD radiation. The jet axis is approximated with the transverse momentum of the leading particle trigger. The observable is defined as

$$j_T = \frac{|\vec{p_t} \times \vec{p_a}|}{|\vec{p_t}|}, \tag{3.1}$$

where $\vec{p_t}$ is the momentum of the trigger particle, while $\vec{p_a}$ is the momentum of the associated particle. Figure 3 illustrates the relation among $\vec{p_t}$, $\vec{p_a}$, j_T, and $x_{||}$, which is defined as the projection of the associated particle's momentum to the direction of the trigger particle's momentum

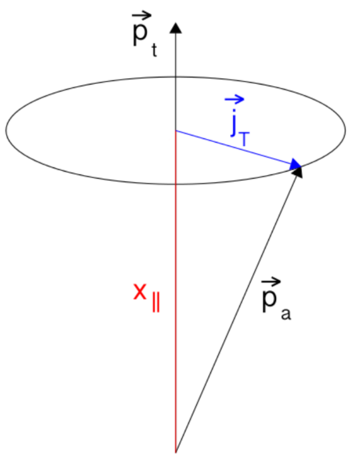

Figure 3: Illustration of j_T and $x_{||}$.

$$x_{||} = \frac{\vec{p_\mathrm{t}} \cdot \vec{p_\mathrm{a}}}{\vec{p_\mathrm{t}}^{\,2}}. \tag{3.2}$$

In this analysis, the near-side is defined as the hemisphere of the trigger particle, $\vec{p_\mathrm{t}} \cdot \vec{p_\mathrm{a}} > 0$. This definition makes the acceptance correction somewhat more complicated as compared to the "traditional" approach, where the near side of the jet is defined as $|\Delta\varphi| < \pi/2$.

From this, one can build up the j_T distribution, with the form

$$\frac{1}{N_\mathrm{trig}}\frac{1}{j_\mathrm{T}}\frac{\mathrm{d}N}{\mathrm{d}\,j_\mathrm{T}} = C_\mathrm{assoc}(p_\mathrm{T,assoc})C_\mathrm{Acc}(\Delta\eta,\Delta\varphi)\frac{N_\mathrm{pairs}(p_\mathrm{T,trig},p_\mathrm{T,assoc},\Delta\eta,\Delta\varphi)}{j_\mathrm{T}N_\mathrm{trig}(p_\mathrm{T,trig})}, \tag{3.3}$$

where N_trig is the number of trigger particles, $N_\mathrm{pairs}(p_\mathrm{T,trig},p_\mathrm{T,assoc},\Delta\eta,\Delta\varphi)$ is the number of particle pairs, C_assoc is the single track efficiency correction and C_Acc is the aforementioned acceptance correction. As in the previously described analysis, the single track efficiency correction was estimated by Monte Carlo simulations, and the mixed event technique was used to correct for the detector acceptance.

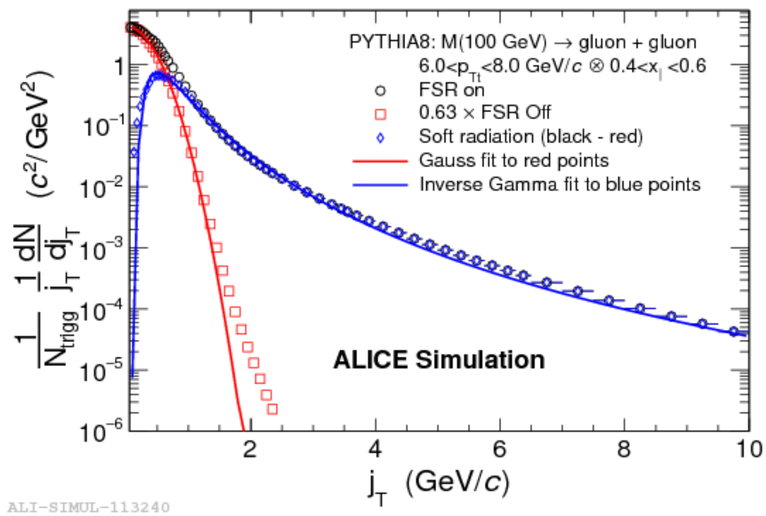

Figure 4: The concept of the two-component model of j_T by a PYTHIA8 study with a di-gluon initial state. Turning the Final State Radiation (FSR) off, one can extract the narrow component. Subtracting that from the total, the wide component of showering becomes visible.

A PYTHIA simulation [7] shows that the j_T distribution can be understood as a sum of two components: the low-j_T is mostly populated by the hadronization described with Lund string model [13] and high-j_T has a tail coming from soft QCD radiation [14]. In this PYTHIA study, events were generated where an artificial resonance particle always decays into two back-to-back gluons that then further shower and hadronize. The results from this simulation are presented as black circles in Fig. 4. If the QCD radiation is turned off in PYTHIA, hadronization only results are obtained, shown as red squares in the same figure. Assuming that the components are additive, the QCD showering part (blue points) is obtained by taking a difference of these two. This study also motivates the choices of the fit functions of these two components to describe the data.

The hadronization part, which is called the narrow component, can be described by a Gaussian

$$f(j_T) = \frac{A_2}{A_1^2} e^{-\frac{j_T^2}{2A_1^2}}, \tag{3.4}$$

while the showering part, the wide component, is best described by the integrand of a gamma function

$$f(j_T) = \frac{A_3 A_5^{A_4-1}}{\Gamma(A_4-1)} \frac{e^{-\frac{A_5}{j_T}}}{j_T^{A_4+1}}, \tag{3.5}$$

where $A_{1..5}$ are the fit parameters. In real data, compared to the PYTHIA simulation, there is an additional background coming from the underlying event. To estimate its contribution, the η-gap method is used, where pairs with $|\Delta\eta| > 1.0$ are considered as background.

The widths were extracted from the fit of the j_T distributions for both the narrow and the wide component. The trigger p_T was in the range of $3 < p_{T,trig} < 15$ GeV/c, and the results are further divided into three $x_{||}$ bins: $0.2 < x_{||} < 0.4$, $0.4 < x_{||} < 0.6$ and $0.6 < x_{||} < 1.0$. The two data sets, pp at $\sqrt{s} = 7$ TeV and p–Pb at $\sqrt{s_{NN}} = 5.02$ TeV are compared to PYTHIA 8 tune 4C in Fig. 5. Further MC comparisons are shown in Fig. 6, where the pp data are compared to the PYTHIA 8 tune 4C and the Monash tune, along with the Herwig LHC-MB tune MC results. The simulations describe the results reasonably well.

The agreement of pp and p–Pb results indicate that there are no cold nuclear effects within uncertainties. The narrow component does not depend on $p_{T,trig}$, supporting the assumption of universal hadronization. All studied models agree. The wide component shows a rising trend with $p_{T,trig}$, which is expected as higher p_T partons tend to have higher virtuality, so they have a larger phase-space for branching, which makes the distribution wider. The same trend can be observed in all the models included. These observations can be used to constrain energy loss models, particularly models that predict broadening of the jet by interactions with the medium.

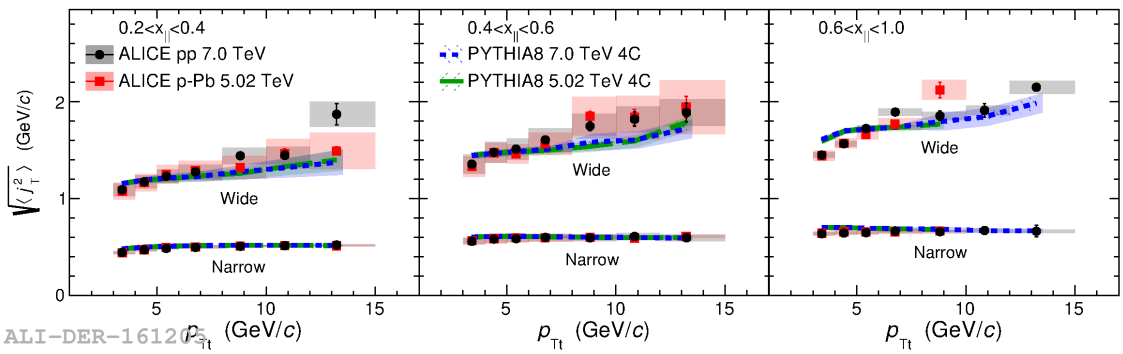

Figure 5: RMS values of the narrow- and wide-component of the j_T distribution. Data are divided into various $x_{||}$ bins ($0.2 < x_{||} < 0.4$ on the left, $0.4 < x_{||} < 0.6$ in the middle and $0.6 < x_{||} < 1.0$ on the right). Black points show results from pp collisions at $\sqrt{s} = 7$ TeV, the red points are from p–Pb collisions at $\sqrt{s_{NN}} = 5.02$ TeV. Both are compared to PYTHIA 8 tune 4C simulations.

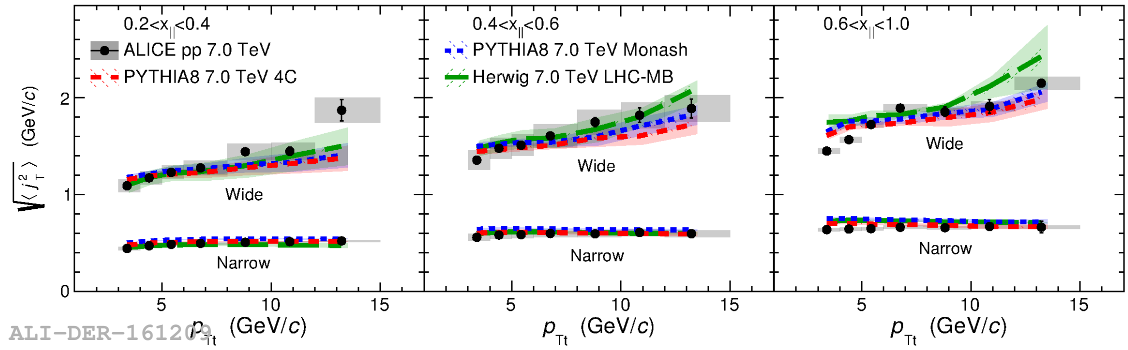

Figure 6: RMS values of the narrow- and wide-component of the j_T distribution. Data are divided into various $x_{||}$ bins ($0.2<x_{||}<0.4$ on the left, $0.4<x_{||}<0.6$ in the middle and $0.6<x_{||}<1.0$ on the right). Black points show results from pp collisions at $\sqrt{s}$ = 7 TeV. Data are compared to PYTHIA8 tune 4C (red line) and Monash tune (blue line) as well as Herwig 7 LHC-MB tune results (green line).

References

[1] A. Majumder and M. van Leeuwen, Prog. Part. Nucl. Phys. **66** (2011) 41

[2] U. A. Wiedemann, Landolt-Bornstein **23** (2010) 521

[3] **STAR** collaboration, G. Agakishiev *et al.*, Phys. Rev. **C85** (2012) 14903

[4] **ALICE Collaboration**, J. Adam *et al.*, Phys. Rev. Lett. **119** (2017) no.10, 102301

[5] **CCOR** collaboration, A. Angelis *et al.*, Phys. Lett. **B97** (1980) 163-168.

[6] **PHENIX** Collaboration, S. S. Adler *et al.*, Phys. Rev. **D74** (2006) 072002.

[7] T. Sjöstrand, S. Mrenna and P. Skands,
JHEP05 (2006) 026,
Comput. Phys. Comm. 178 (2008) 852.

[8] M. Bahr *et al.*, Eur. Phys. J. C **58**, 639 (2008)

[9] J. Bellm *et al.*, Eur. Phys. J. C **76**, no. 4, 196 (2016)

[10] **PHENIX** Collaboration, S. S. Adler *et al.*, *Phys. Rev.* **C73** (2006), 054903

[11] **CDF** Collaboration, A. Angerami, *Phys. Rev. Lett.* **102** (2009) 232002.

[12] **ATLAS** Collaboration, A. Angerami, J. Phys. G38 (2011) 124085.

[13] B. Andersson, G. Gustafson, G. Ingelman and T. Sjöstrand, Phys. Rept. **97** (1983) 31.

[14] Y. L. Dokshitzer, V. A. Khoze, A. H. Muller, S. I. Troian,
Basics of Perturbative QCD, Editions Frontieres, Gif-sur-Yvette, France, 1991.